Improvement of Hydriding Properties of Ti-Cr Based Hydrogen Absorbing Alloys Developed for An MH Refrigerator

Toshiki KABUTOMORI*, Toshio TAKAHASHI*, Harunobu TAKEDA*
and Yuichi WAKISAKA*

—Synopsis—

Hydrogen absorbing alloys were developed fbr an F-class MH refigerator. A $TiCr_2$ alloy was employed for the system, and by substitution of Zr for Ti and of Fe for Cr in the alloy, hydrogen equilibrium dissociation pressure could be controlled freely in the range fom room temperature to 183 K. Moreover, substitutiono of Mn for Cr, addition of a small amount of Cu and optimum heat treament made it possible to fiatten the plateau slope in P-C-T curves.

Examination of cyclic properties and hydriding kinetics of the alloys at a lower temperature revealed sufficient hydriding kinetics with full hydrogen absorbing time within 5 min at 183 K and
superior life cycle with a degradation ratio of 10% after 50,000 absorption/desorption cycles. Furthermore,a prototype refrigerator was made using the developed hydrogen absorbing alloys and the performance of the device was investigated. It was confirmed that refrigeration output of the 243 K class could be obtained.

1. Introducttion

Recently driven by the global environmental issues, the regulation for using flon, one of environment destroying materials, is being strengthened. In response to this, efforts for developing alternate machines for compression heat pump using flon have been eagerly made. In the area of air conditioning in close vicinity of the normal temperatures, compression heat pumps using substitute flon and absorption heat pumps based on various substances have been commercialized. For the lower temperature range[1], below 253 K, so-called F-class refrigeration range, however, there is not an appropriate working medium, and currently, attempts are being made to replace the flon-based refrigerating machine with those based on ammonia absorption refrigeration[2], and on MH refrigeration using hydrogen absorbing alloys[3].

While ammonia-based refreigerating machines had been used from earlier time than the flon-based refrigerators, the use of ammonia-based machine is limited owing to some demerits of ammonia, such as strong corrosiveness to make the machine design difficult, and high toxicity in the event of leakage. On the other hand, the MH refrigerator is much more attractive for the refrigerator users despite the use of explosive hydrogen, because of enhanced safety due to hydrogen storage in alloys and sealed container, operation in relatively lower pressure range (<1 MPa) and clean nature of hydrogen energy. The MH refrigerator is a sort of heat pump which generates 'cold heat' by utilizing heat of chemical reaction associated with the hydrogen absorption/desorption in the alloys, and the equilibrium characteristics of hydrogen-alloy reaction is requested to meet the necessary cold heat output. Particularly, in case of F-class refrigerator with cold heat output ranging from 250 K to 210 K, the hydriding equilibrium properties of alloys are required to have an equilibrium dissociation pressure around 0.1 MPa in that temperature range.

A number of hydrogen absorbing alloys have been developed to cover diverse applications. These alloys may be classified into three types, according to their crystalline structures and relative compositions: (1) AB_5 alloys represented by $LaNi_5$[4], (2) AB alloys such as TiFe[5], and (3) AB_2 alloys of C14 Laves phase structure such as $TiMn_{1.5}$[6]. Among these alloys, AB_5 and AB groups have the equilibrium dissociation pressure located in a range from the normal temperature to 373 K or so, and based on the previous experience, it seems difficult to shift the equilibrium dissociation pressure to a range of lower temperatures by replacing component elements one with another. On the other hand, in case of AB_2 alloys, some promising

*Muroran Research Laboratory

combinations may be available by pairing transition metals with Zr or Ti[7,8]. Particularly, alloys based on combination of transition metals with Ti may be regarded to have the equilibrium dissociation pressure in a range from the normal temperature toward the lower side. Of these, $TiMn_{1.5}$ alloy, which has C14 Laves phase structure and contains Ti richer than the stoichiometric composition, has been intensively studied for understanding the basic hydriding properties[10] and for testing the effects of adding various elements[11], owing to its equilibrium dissociation pressure around 0.1 MPa at 253 K[6] and adequate effective hydrogen moving capacity at the plateau as well as excellent plateau characteristics[9]. While the $TiMn_{1.5}$ alloy has larger hysteresis in respect to hydrogen absorption and desorption pressures, which could be little improved by changing substitute elements, it may be regarded as an alloy of good hydriding properties in overall assessment, including less aging than the AB_5 alloys after repeated cycles of absorption/desorption[12]. In case of $TiCr_2$ alloy[13], which is of the same C14 Laves phase structure as $TiMn_{1.5}$, the equilibrium dissociation pressure is 0.1 MPa at temperature as low as 213 K, which is suited for the refrigerating heat pump to generate cold heat ranging from 250 K to 210 K. Though $TiCr_2$ has hydrogen storage capacity comparable to that of $TiMn_{1.5}$, With $H/M = 1$ at temperature 213 K and 5 MPa hydrogen pressure, its effective hydrogen moving capacity at the plateau of the P-C-T curve is as poor as $H/M = 0.5$ (110 cc/g), suggesting reduced efficiency when installed in a refrigerating machine. Besides, the equilibrium dissociation pressure is too high for the refrigerator application, requiring specific control of equilibrium dissociation pressure depending upon the refrigerating output.

The present report concerns the development of $TiCr_2$-based alloys for the purpose of accomplishing adequate control of equilibrium dissociation pressure characteristics and augmenting the effective hydrogen capacity at the plateau of P-C-T curve, in consideration of applying the $TiCr_2$ alloys to the F-class MH refrigerator. Moreover, the report includes the characterization of reactivity and durability in the lower temperature range for assessing the reliability of resultant alloys in the actual working environment, and the performance evaluation of trial-manufactured prototype refrigerator.

2. Experimental Methods

2.1 Specimens

Specimens used for testing consisted of quaternary alloys, $Ti_{1-x}Zr_xCr_{2-y}Fe_y$ with Ti partly replaced with Zr and Cr partly with Fe, five-element alloys, $Ti_{1-x}Zr_xCr_{2-y-z}Fe_yMn_z$ with Cr replaced further partly with Mn, and two types of five-element alloy, $Ti_{0.7}Zr_{0.3}Cr_{1.3}Fe_{0.3}Mn_{0.4}$ and $Ti_{0.4}Zr_{0.6}Cr_{1.2}Fe_{0.4}Mn_{0.4}$, with Cu added at a dose of $Cu_{0.05}$ to $Cu_{0.5}$ to check the effect of Cu-doping. Raw materials for the specimens were sponge titanium and sponge zirconium of 99.8 % purity; electrolytic nickel, iron and manganese of nominal purity 99.9%; and pure copper of purity 99.999%. Alloys were melted by arc melting in a water-cooled copper crucible in argon atmosphere (0.04 MPa). Most of specimens were of truncated cone shape with 30 mm diameter and 10 mm height, weighing about 50 g. After having melted, the specimen underwent a homogenizing heat treatment under 0.1 MPa Ar gas atmosphere at 1573 K for 10 hours, to ensure homogeneous alloy composition. For some specimens, the duration and temperatures of heat treatment were varied. Following the heat treatment, the specimen was crushed into powder of 48 to 200 mesh and used for the measurement of hydrogen storage characteristics, X-ray diffraction and ICP analysis. It was verified through the ICP analysis of melted specimen that the final specimens attained the target composition.

2.2 Measurement of Hydriding Equilibrium Characteristics

For evaluating the hydriding characteristics of specimen, the P-C-T curves were measured, to determine the equilibrium pressure properties, effective hydrogen capacity, slope of plateau and hysteresis. A flow chart of the characterization is given in **Fig. 1**. The procedure of specimen initial activation consists of sealing 5 g specimen in a reaction container, keeping it in a temperature bath at 353 K, and evacuating for 1 hour. Then, the reaction container is kept in a bath of specified temperature (193 K to 293 K), and hydrogen is fed into the container at a pressure of 5 MPa. After these steps, most of specimens start to absorb hydrogen as soon as it is fed in, attaining a steady state in 10 minutes or so. When the absorption is stabilized, the evacuation is resumed to desorb hydrogen at 353 K, and then, hydrogen is allowed to be absorbed again at a lower temperature. This cycle is repeated for 2 to 3 times to finish the initial activation. Then, the P-C-T curves are recorded at a specified temperature. For each of specimens, the measurement was made at three or more different temperature conditions, using commercially available hydrogen of nominal purity 99.99999% and

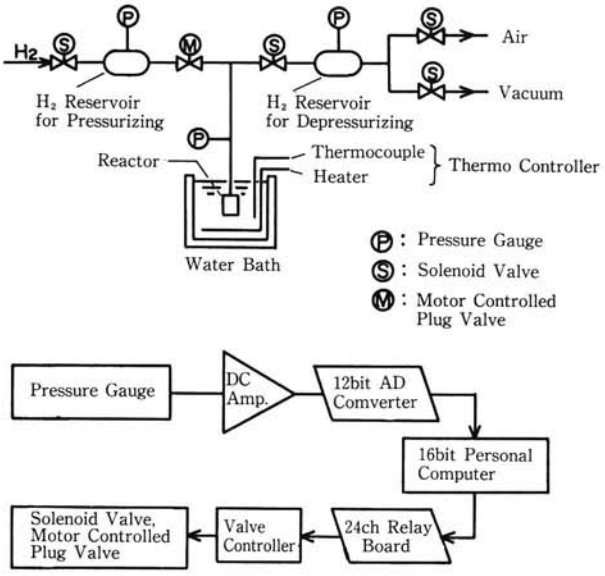

Fig. 1 Flow chart of pressure-composition-isotherm (P-C-T) measuring setup

dew-point temperature 203 K or lower.

2.3 Determination of Reaction Rate

Alloys used for determining reaction rate consisted of $Ti_{0.9}Zr_{0.1}Cr_{1.6}Fe_{0.4}$ with equilibrium dissociation pressure 0.1 MPa at 203 K. In order to minimize changes in alloy temperatures due to heat conduction and reaction heat, each of specimens was composed of 0.2 g alloy and 0.8 g Ni powder. For ensuring good heat conduction between specimen and container, the specimen holder of the container was made from Cu, and a cylindrical block of Cu was placed on mounted specimen powder to improve the contact between the specimen and the container. The reaction rate was measured with a particular alloy by applying various hydrogen pressures at temperatures ranging from 183 K to 213 K, to evaluate quantitatively the effects of temperature and hydrogen pressure.

2.4 Durability Test

Alloys $Ti_{0.9}Zr_{0.1}Cr_{1.6}Fe_{0.4}$ were used for the evaluation of durability. The test was carried out through the pressure cycle method to repeat absorption and desorption of hydrogen by repeated augmentation and reduction of hydrogen pressure at a fixed temperature. An alloy specimen 1 g is mounted in a reaction container, evacuated and allowed to fully absorb hydrogen and stabilize through the initial activation procedures. The pressure level for the cycle test was set on the basis of the P-C-T curve recorded for particular cycle test temperatures, so that the absorption pressure might be adequately higher than the pressure at the end point of plateau, and the desorption pressure adequately lower than that at the beginning of plateau. A cycle time was about 4 minutes: 2 min for absorption and 2 for desorption. For all the specimens, it was confirmed that the reaction was completed within this time. For the durability test, commercially available hydrogen of nominal purity 99.99999 % and dew-point temperature 203 K or lower was used.

3. Results and Discussion

3.1 Effects of Partial Replacement of Ti with Zr and of Cr with Fe and Mn in $TiCr_2$ Alloys

In case of $Ti_{1-x}Zr_xCr_{2-y-z}Fe_yMn_z$ alloys derived from $TiCr_2$ alloys by partly replacing Ti with Zr, and Cr with Fe and Mn, it was found that the alloys were of single phase C14 structure through the phase analysis based on X-ray diffraction, so long as the replacement met the following conditions: $0<x<1.0$, $0<y<1.0$ and $0<z<0.5$. The lattice parameters a and c of the C14 crystal structure tended to increase on replacement with Zr and Mn, and to decrease on replacement with Fe.

Fig. 2 shows a P-C-T diagram of $TiCr_{2-y}Fe_y$ derived by partly replacing Cr with Fe and recorded at 213 K. In $TiCr_{1.8}Fe_{0.2}$ alloy with 10% of Cr replaced with Fe, the equilibrium dissociation pressure was lower than that of $TiCr_2$, while if more than 10% of Cr was replaced with Fe, the pressure tended to increase with the degree of replacement. The width of plateau, which was $\Delta H/M = 0.4$ or so in $TiCr_2$ alloy, tended to steeply increase with the proportion

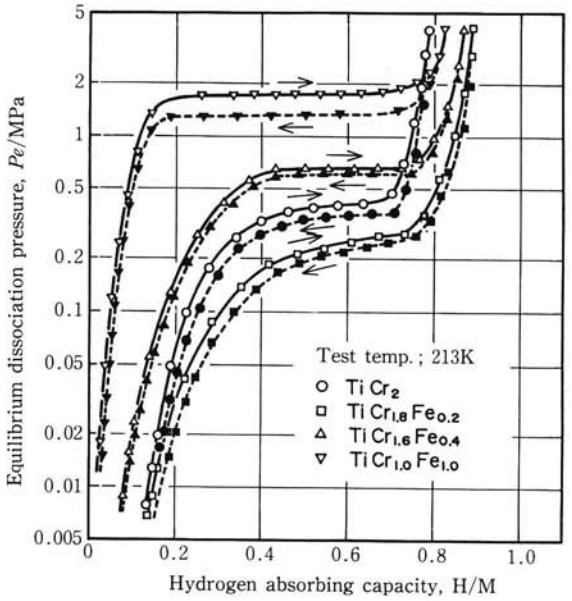

Fig. 2 P-C-T diagrams of the $TiCr_{2-y}Fe_y$ alloys

of replacement with Fe. The starting point of the plateau, which was not so clear in $TiCr_2$ alloy, became clearly recognizable with increasing accuracy as Cr was replaced by Fe at an growing proportion. **Fig. 3** shows P-C-T diagrams of $TiCr_{1.4}Fe_{0.6}$ alloys with Ti partly replaced by Zr. When Ti was partly replaced with Zr in alloys $TiCr_{1.4}Fe_{0.6}$ the following trends were recognized: the equilibrium dissociation pressure at the plateau was lowered, the slope of the plateau became steeper, and the hydrogen storing capacity at 5 MPa increased.

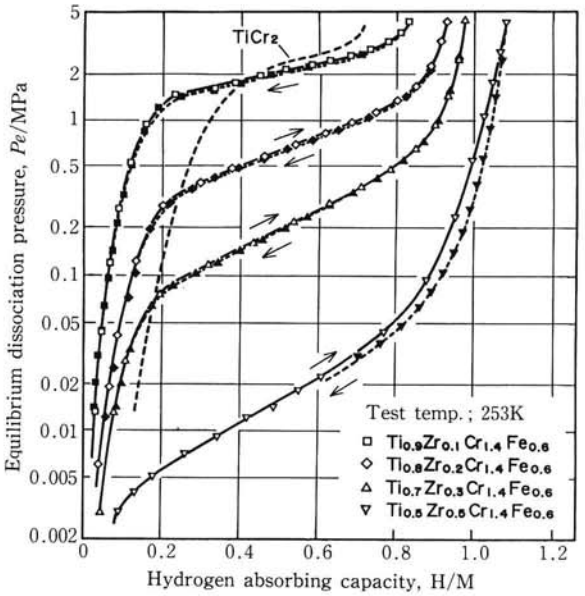

Fig. 3 P-C-T diagrams of the $Ti_{1-x}Zr_xCr_{1.4}Fe_{0.6}$ alloys

On the basis of these results, it may be concluded that $TiCr_2$ alloys with Ti partly replaced with Zr have the equilibrium dissociation pressure lower than that of $TiCr_2$ and the plateau width greater. The alloys with Cr partly replaced by Fe have the equilibrium dissociation pressure raised and the extent of plateau increased as in case of replacing Ti with Zr. The trend of making the plateau slope steeper by replacement with Zr can be reversed by the partial replacement of Cr with Fe. In this way, simultaneous partial replacements with Zr and Fe seem to have a potential of compensating demerit of individual replacement, to enlarge the plateau extent and to control the equilibrium dissociation pressure arbitrarily.

Fig. 4 shows the effects of simultaneous partial replacement of Ti with Zr, and Cr with Fe in $TiCr_2$ to the equilibrium dissociation pressure of the alloy, which provide a master guide for looking for the alloy composition to realize the target equilibrium dissociation pressure. **Fig. 5** shows the relationship of

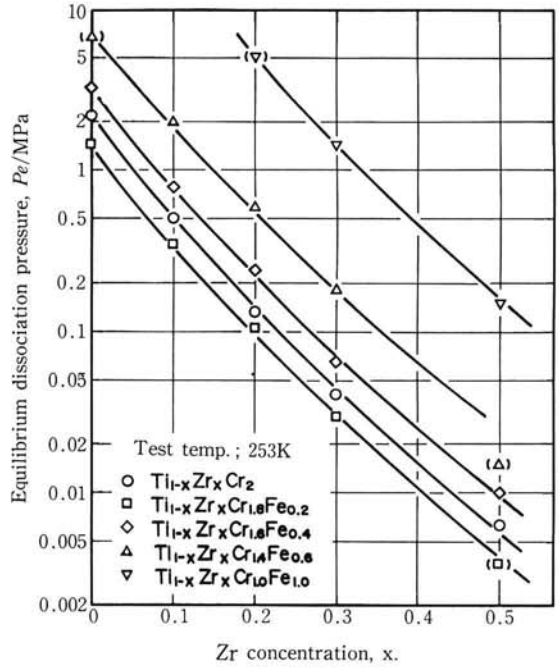

Fig. 4 Eflect of the Zr concentration on the equilibrium dissociation pressure at the center of plateau on P-C-T curves of the $Ti_{1-x}Zr_xCr_{2-y}Fe_y$

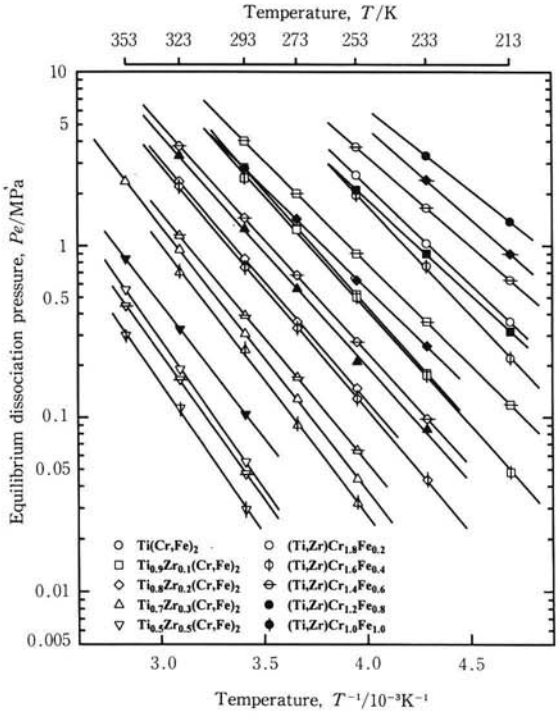

Fig. 5 Equilibrium pressure-temperature(P-T) diagrams of the $Ti_{1-x}Zr_xCr_{2-y}Fe_y$ alloys

equilibrium dissociation pressure to temperature (P-T diagram) derived from P-C-T diagrams of $Ti_{1-x}Zr_xCr_{2-y}Fe_y$ alloys, where x =0~0.5 and y = 0~1.0.

Table 1 Eathalpy change ΔH and entropy change ΔS in hydriding reaction of $Ti_{1-x}Zr_xCr_{2-y}Fe_y$ alloys, (upper side; $\Delta H/kJ(molH_2)^{-1}$, lower side; $\Delta S/J(molH_2 \cdot K)^{-1}$)

	$Ti_{1-x}Zr_xCr$	$Ti_{1-x}Zr_xCr_{1.8}Fe_{0.2}$	$Ti_{1-x}Zr_xCr_{1.6}Fe_{0.4}$	$Ti_{1-x}Zr_xCr_{1.4}Fe_{0.6}$	$Ti_{1-x}Zr_xCr_{1.0}Fe_{1.0}$
$TiCr_{2-y}Fe_y$	−22.36 −115.2	−22.78 −114.5	−20.11 −109.5	−18.59 −108.7	——
$Ti_{0.9}Zr_{0.1}Cr_{2-y}Fe_y$	−24.61 −110.8	−25.87 −115.6	−23.03 −109.3	−21.16 −108.7	——
$Ti_{0.8}Zr_{0.2}Cr_{2-y}Fe_y$	−27.16 −10.2	−27.56 −111.1	−24.79 −107.1	−22.91 −105.8	−19.80 −111.1
$Ti_{0.7}Zr_{0.3}Cr_{2-y}Fe_y$	−29.78 −110.0	−30.40 −110.9	−28.28 −107.8	−25.94 −109.4	−21.80 −108.7
$Ti_{0.5}Zr_{0.5}Cr_{2-y}Fe_y$	−32.28 −105.5	−23.47 −104.5	−31.46 −101.8	−29.92 −102.4	−26.71 −108.1

For all of the alloys, P-T diagrams are nearly linear, demonstrating the Van't Hoffs relation. Values of enthalpy change ΔH and entropy change ΔS of hydrogen at the time of hydride formation as calculated from the Van't Hoffs relation are given in **Table 1**. The absolute value of enthalpy change in $Ti_{1-x}Zr_xCr_{2-y}Fe_y$ alloys tends to increase with addition of Zr and to decrease with addition of Fe. In other words, hydride is stabilized more by adding Zr and less by adding Fe. These trends are in line with those in equilibrium dissociation pressure: the addition of Zr stabilizes hydride and shifts the equilibrium dissociation pressure to the higher temperature side, while the addition of Fe makes hydride less stable and displaces the equilibrium dissociation pressure to the lower temperature side.

Fig. 6 shows P-C-T diagrams of $Ti_{0.5}Zr_{0.5}Cr_{1.7}Fe_{0.3}$ alloy and that with Cr partly replaced by $Mn_{0.5}$ In the alloy $Ti_{0.7}Zr_{0.3}Cr_{1.7}Fe_{0.3}$, the slope of plateau in the P-C-T characteristics is so steep as to make the plateau indistinct. If Cr is partly replaced with $Mn_{0.5}$, the plateau in P-C-T diagram turns more distinct with its slope reduced. Increasing the Mn dose tends to augment the hydrogen storing capacity. For the equilibrium dissociation pressure characteristics, while the plateau is not so clear as to make it difficult to identify the mid-point of plateau in alloys without including Mn, the partial replacement of Cr with Mn reduces the equilibrium dissociation pressure when compared at the mid-point of plateau where hydrogen is desorbed to a half of its storage capacity.

It has been reported that the stability of hydride of AB_5 alloys depends upon the size of interstitial space in the crystal lattice which is supposed to be occupied by hydrogen[14]. In the C14 Laves phase structure, on the other hand, it has been confirmed on the basis of structural analysis of deuteride of $TiMn_{1.5}$ alloys[9], that a hydrogen atom occupies an

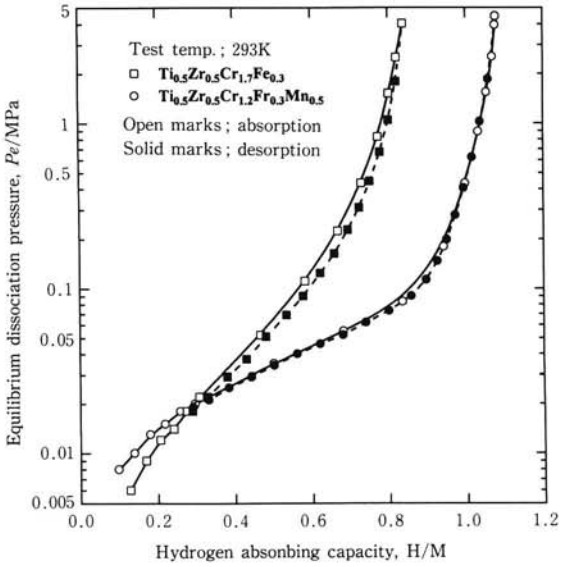

Fig. 6 P-C-T diagrams of $Ti_{0.5}Zr_{0.5}Cr_{1.7}Fe_{0.3}$ alloys and that with Cr partly replaced by $Mn_{0.5}$

A_2B_2 tetrahedral site surrounded by two Ti atoms and two Mn atoms. A unit cell of C14 structure is found to contain four kinds of tetrahedral site, in which the presence of deuterium is confirmed. In order to check the stability of $TiCr_2$ alloy hydride, the size of interstitial space site to be filled by a hydrogen atom within a crystal was determined by using a rigid sphere model. Based on X-ray diffraction patterns, exact structural parameters were determined by using Rietveld's analysis[15], and the radius of sphere inscribed to A_2B_2 tetrahedral lattice space surrounded by two Ti atoms and two Cr/Fe atoms was calculated. For the radius of metal sphere in the lattice, Goldschmidtls radius was used. **Fig. 7** shows the relation of obtained site size to reaction heat. The reaction heat ΔH of hydriding has been recognized to be in close correlation with the size of

interstitial site to be filled by hydrogen: the larger the interstitial space is, the greater the reaction heat grows, making hydride more stable. In considering partial replacement of Cr by Fe or Mn in $TiCr_2$ alloys, it should be noted that the radius of Fe atom 1.27 Å is slightly smaller than that of Cr atom 1.28 Å, and that of Mn atom 1.30 Å is larger than the latter. For this reason, when Cr is replaced with Fe, the size ofcrystal lattice and interstitial space is reduced, to make hydride less stable, while the replacement with Mn causes a reverse effect. In specimens with Ti partly replaced with Zr, the lattice parameters tend to increase, because the radius of Zr atom 1.60 Å is larger than that of Ti atom 1.47 Å. The increment of lattice volume seemingly increases the size of interstitial space, and consequently, thereplacement with Zr stabilizes hydride.

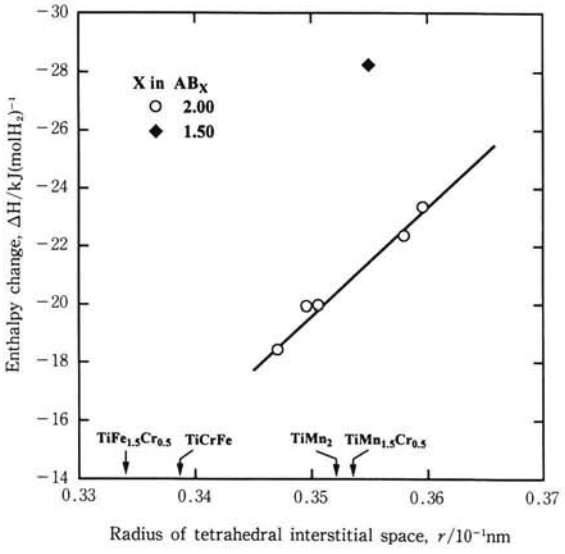

Fig. 7 Relation of radius of tetrahedral interstitial space to enthalpy change ΔH

3.2 *Effects of Cu Addition and Heat Treatment to Slope of Plateau*

Partial replacement of Ti with Zr in $TiCr_2$ alloys tends to increase the plateau slope, which may be compensated by replacing Cr partly with Fe and Mn to some extent, but not adequate for the practical applications. For this reason, the effects of adding a small amount of Cu and homogenizing heat treatment was studied in $(TiZr)(CrFeMn)_2$ alloys which are derived from $TiCr_2$ by partly replacing Ti with Zr, and Cr with Fe and Mn. **Fig.** 8 shows changes in plateau slope of P-C-T diagram when changing the dose of Cu addition to $Ti_{0.7}Zr_{0.3}Cr_{1.3}Fe_{0.3}Mn_{0.4}Cu_x$ and $Ti_{0.4}Zr_{0.6}Cr_{1.2}Fe_{0.4}Mn_{0.4}Cu_x$ alloys. In these two alloys,

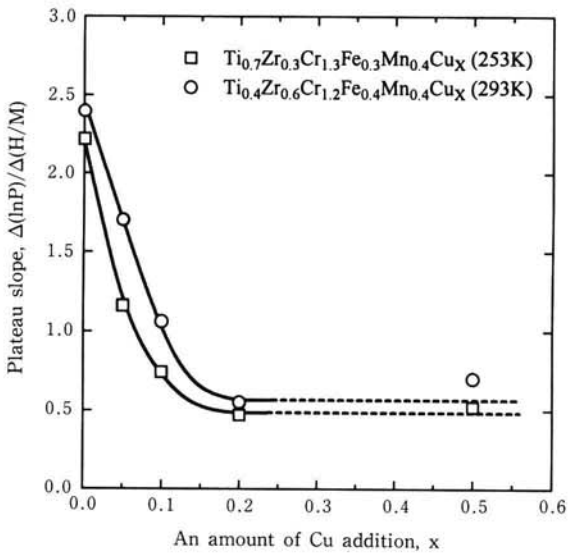

Fig. 8 Eflect of an amount of Cu addition on plateau slope of P-C-T diagrams of $Ti_{0.7}Zr_{0.3}Cr_{1.3}Fe_{0.3}Mn_{0.4}Cu_x$ and $Ti_{0.4}Zr_{0.6}Cr_{1.2}Fe_{0.4}Mn_{0.4}Cu_x$ alloys

the effects of adding Cu presented nearly identical trends.. the plateau slope falls steeply up to $Cu_{0.15}$, and then becomes nearly unchanged on further increasing Cu dose. In this way, it is evident that in $(TiZr)(CrFeMn)_2$ alloys the slope of plateau in P-C-T diagram can be effectively reduced by adding Cu. It should be noted, however, that adding Cu too much may reduce the hydrogen storage capacity. The optimum dose of Cu seems to be $Cu_{0.1}$, Where the hydrogen storing capacity is not affected so much, while the slope of plateau is improved markedly.**Fig.9** shows the slope of plateau in $Ti_{0.4}Zr_{0.6}Cr_{1.2}Fe_{0.4}Mn_{0.4}Cu_{0.05}$ alloy after the heat treatment for varied period at 1573 K, and that for 10 hours at various temperatures. While the heat treatment at temperatures up to 1573 K or for period up to 10 hours affected the plateau slope very little in comparison to AS materials, raising the temperature or extending the period of heat treatment markedly contributed to reducing the slope. The heat treatment at 1573 K for 100 hours gave nearly identical effects as that for 10 hours at 1473 K. On the basis of these results, it may be concluded that the heat treatment, and particularly, the temperature of heat treatment is highly effective for improving the plateau slope of $TiCr_2$ alloys added with Zr.

The slope of plateau in the P-C-T diagram in hydrogen absorbing alloys seems to be attributable basically to inhomogeneity in alloy composition. The fluctuation in alloy composition may cause that in the

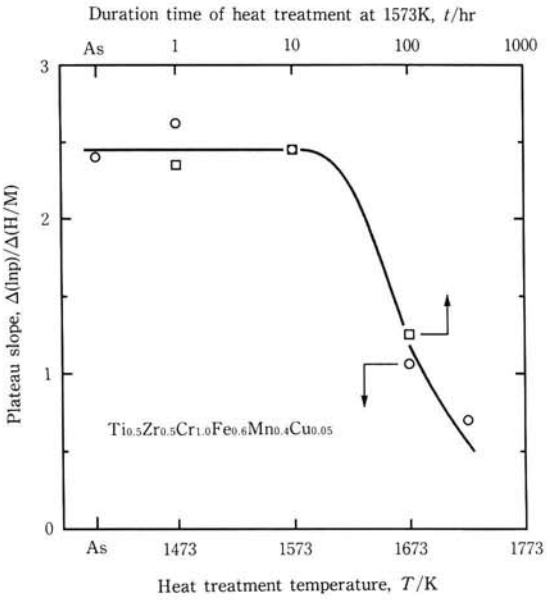

Fig. 9 Eflect of hert treatmemt conditions on the plateau slop of $Ti_{0.5}Zr_{0.5}Cr_{1.0}Fe_{0.6}Mn_{0.4}Cu_{0.05}$ alloys

stability of hydride, which is redected in the plateau slope of P-C-T diagram. In case of $TiCr_2$ alloys, atoms of two component elements are regularly arranged with very little fluctuation to minimize the plateau slope in P-C-T diagram. On the other hand, in 3-, 4- or 5-element alloys derived from $TiCr_2$ with Ti partly replaced by Zr, and Cr partly by Fe or Mn, it may be natural that local inhomogeneity occurs owing to different replacement of microscopic extent through the compositional fluctuation in melting and the preferential sedimentation of stabilized elements in the process of condensation. It seems that microscopic difference in composition, that is, the fluctuation in replacement elements, contributes to the plateau slope of P-C-T diagram.

Cr, Fe and Mn constitute transition metal of valence 3, of which atoms have similar properties and nearly identical Goldschmidt's radius, ensuring homogeneous replacement. As shown in **Fig. 4** the effects of replacement with these elements to the equilibrium dissociation pressure are less pronounced than those of replacement with Zr. In the latter case, as Ti belongs to a period different from that of Zr, and the radius of Ti is considerably different from that of Zr the replacement seems to proceed not so smoothly. Moreover, the effect of replacement with Zr to the equilibrium dissociation pressure is much greater than that with Fe, and with the same amount of compositional fluctuation, the plateau slope in P-C-T diagram is affected more profoundly with Zr than with Fe. For this reason, the replacement with Zr seems to increase the slope of plateau. It has been found that the partial replacement of Cr with Mn and the addition of a small amount of Cu is effective for reducing the plateau slope. The X-ray diffraction pattern of $Ti_{0.4}Zr_{0.6}Cr_{1.2}Fe_{0.4}Mn_{0.4}Cu_x$ alloys indicates that the greater the dose of Cu is, the sharper becomes the peak, indicating that the addition of Cu makes the compositional distribution of Zr more homogeneous.

While it is not known certainly, why the addition of Mn or Cu improves the homogeneity of composition, the melting point of six kinds of AB_2 type intermetallic compounds is shown in **Table 2**, as obtained by the combination of Ti or Zr with Cr, Mn and Fe[16]. The melting point of intermetallic compounds involving Zr is 100 K to 300 K higher than those involving Ti, and it seems that Zr-rich phase of higher melting point precipitates first in the process of condensation, causing inhomogeneous composition. On the contrary, melting point of alloys including Cr-Fe- Mn have minor difference, the precipitation at the time of condensation seems to occur nearly simultaneously. The heat treatment is supposed to bring forth homogeneous distribution of composition through the mutual diffusion of component elements. Since the diffusion involves time or temperature as parameters, its progress is extended by prolonging time or raising temperature. This fact is demonstrated in Fig. 9, indicating that the diffusion advances with time or rise of temperature, resulting in homogeneous composition.

Table 2 Melting points of C14 Laves phase alloys

Alloy	Melting Point, K
$TiCr_2$	1370
$TiFe_2$	1427
$TiMn_2$	1325
$ZrCr_2$	1673
$ZrFe_2$	1673
$ZrMn_2$	1450

3.3 Evaluation of Reaction Rate

Fig. 10 shows changes in the reaction rate on varying the initial hydrogen pressure at temperatures 183 K and 203 K. At either temperature, the higher the initial pressure is, the greater becomes the reaction rate, showing marked dependence on hydrogen pressure. When the difference between the initial hydrogen pressure and the equilibrium pressure is

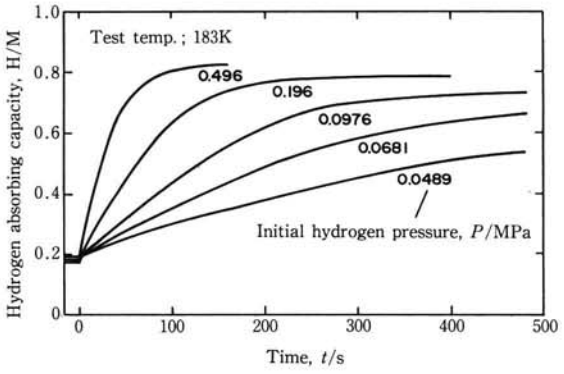

(a) Results at temperature of 183K

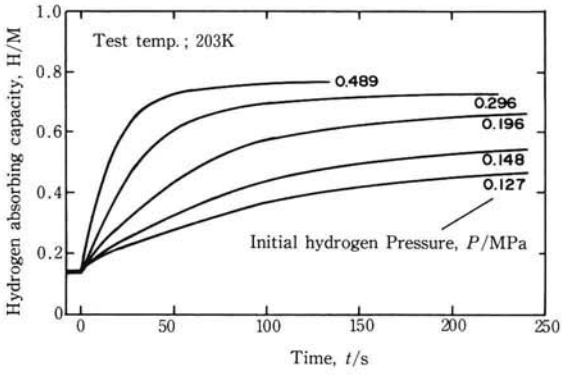

(b) Results at temperature of 203K

Fig. 10 Reaction rate on varying the initial hydogen pressure at temperatures of 183K and 203K

identical, the higher the testing temperature is, the greater the reaction rate becomes, demonstrating the temperature dependence of reaction rate.

On the basis of these results, it was attempted to describe quantitatively the reaction rate of these alloys for the purpose of understanding the reaction dynamics of hydrogen storing alloys at lower temperatures in view of the practical applications, assessing the performance of the actual system and reflecting the findings in the equipment design. The quantitative description of reaction rate has been available with $LaNi_5$[17,18], $TiFe$[19], $ZrMn_2$ and $TiMn_{1.5}$ alloys[20], a number of models have been proposed based on the dependence on hydrogen concentration (hydriding rate) in regard to the reaction mechanism and the rate-determining process. For the purpose of formulating the reaction rate in $Ti_{0.9}Zr_{0.1}Cr_{1.6}Fe_{0.4}$ and for identifying the rate-determining process, the rate equation involving parameters of dependence on pressure, temperature and hydrogen concentration is studied. The reaction rate obtained by the analysis is shown in Eq. (1).

$$df(F)/dt = k\cdot\{-\ln(1-F)\}^{2/3}(1-F)\cdot\exp(-Q/RT)\cdot(P^{1/2}-Pe^{1/2})\cdots(1)$$

The equation for reaction is obtained by integrating Eq. (1):

$$\{-\ln(1-F)\}^{1/3} = K\cdot\exp(-Q/RT)\cdot(P^{1/2}-Pe^{1/2})\cdot(t-t_0)\ \cdots\cdots\cdots(2)$$

where reaction fraction F is given by $F = 0.85/(H/M)$ as the hydrogen absorbing capacity is $H/M = 0.85$ or so. The second term of Eq. (1) represents dependence on hydrogen concentration, the third term that on temperature, and the fourth term that on hydrogen pressure. In Eq. (2), the rate constant is $K = 180.02\ MPa^{1/2}$, and the activation energy is $Q = 14.15$ kJ/molH_2K.

The rate constant of hydriding reaction in $Ti_{0.8}Zr_{0.1}Cr_{1.6}Fe_{0.4}$ obtained by the present study is given in **Fig. 11** together with those reported by other authors. It should be noted that simple comparison is not justified because other authors' data are expressed in different format and rate constants have different dimensions, and the expression of rate constant includes a term depending upon the grain size of alloy powder, or reaction surface area. The alloy powder used in this study has grain size of about 20 μm after the end of testing, not so finer in comparison to other alloy systems. The reaction-time curves at around the room temperature for $TiFe_{0.8}Mn_{0.2}$ alloy reported by Lee et al.[21], and those for $Ti_{0.8}Zr_{0.1}Cr_1Mn_1$ studied by Shitikov et al.[22], the completion of the reaction takes 60 seconds or longer under every condition, much longer than the reaction shown in **Fig. 10**. On

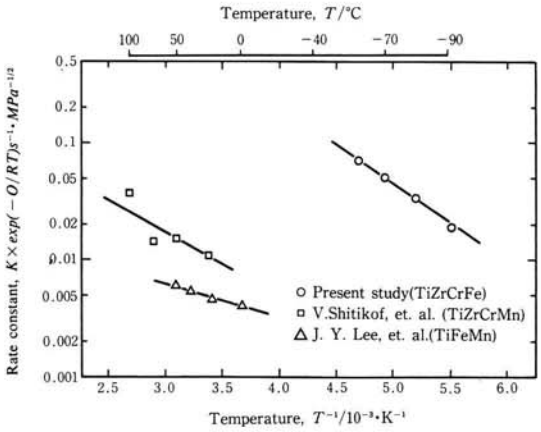

Fig. 11 Comparison of rate constants in several kinds of hydrogen storage alloy

the basis of these facts, it may be stated that the reaction is fast enough at temperatures as low as 200 K.

3.4 Evaluation of Durability

Fig. 12 shows the characteristics of cyclic absorption/desorption of hydrogen of $Ti_{0.9}Zr_{0.1}Cr_{1.6}Fe_{0.4}$

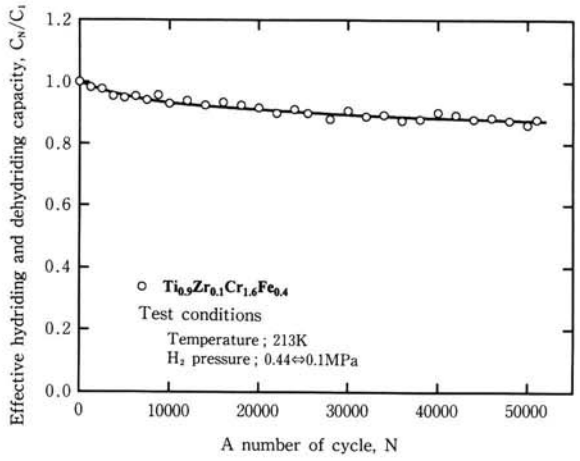

Fig. 12 Durability of $Ti_{0.9}Zr_{0.1}Cr_{1.6}Fe_{0.4}$ alloy

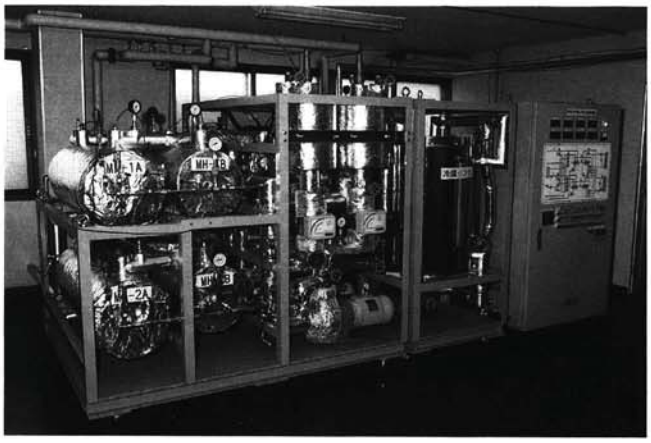

Photo 1 External photograph of MH retrigerator

alloy at 213 K. The amount of hydrogen absorbed and desorbed gradually decreases as the number of cycles grows: the amount of hydrogen absorption/desorption is reduced to 90% of the initial value after the repetition of about 50,000 cycles, aging by 10%. This indicates that the alloy has much better duration in comparison to alloys of relatively extensive aging, such as AB_5 alloys[23,24].

The mean grain size of specimen alloy powder after the cyclic test was 20 μm or so, indicating that the alloy is adequately resistant to pulverizing effect of hydriding.

4. Application of Resultant Alloys to Refrigerating System[25]

It was attempted to apply alloys developed in this study to the actual refrigerating system for examining the performance of the system. The machine is of heat-driven heat pump type, in which heat is produced by exchanging hydrogen between two kinds of hydrogen storing alloy. The system can produce "cold heat" of 243 K at a rate of 10,000 kcal/h. The refrigerating system consists of two MH reaction containers for generating cold heat, and two MH reaction containers for regulating hydrogen pressure. An outer view of the refrigerating system is shown in **Photo 1**. The reaction container is of shell and tube construction, with alloys mounted in a tube of inner diameter 10.5 mm. In the reaction container for producing cold heat, $Ti_{0.73}Zr_{0.27}Cr_{1.3}Fe_{0.3}Mn_{0.4}Cu_{0.05}$ alloy of optimized design was mounted, which had 0.1 MPa equilibrium dissociation pressure at 253 K. **Fig. 13** shows P-C-T diagrams of this alloy at 253 K and 303 K. For each of reaction containers, 60 kg

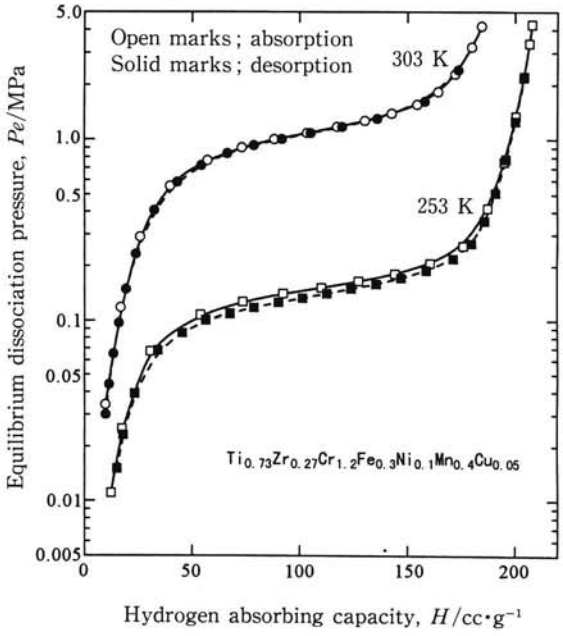

Fig. 13 P-C-T diagrams of the alloy used for MH refrigerator

alloy was used under an assumption that alloy for refrigerating can adsorb/desorb hydrogen at 120 cc/g capacity and operation rate is 3 cycles per hour.

The refrigerating system shown in **Photo 1** was installed in a 10,000 kcal/h class refrigerator of about 100 m^3 inner capacity to check the refrigerating output. Changes in the refrigerator temperature after starting the operation is shown in **Fig. 14**. As the operation was started, the inside temperature was gradually lowered down to 243 K in 11 hours. The temperature ot hydrogen absorbing alloy was found to be 235 K at this time. On the basis of these results, it was demonstrated that $(TiZr)(CrFeMn)_2Cu_x$ alloys

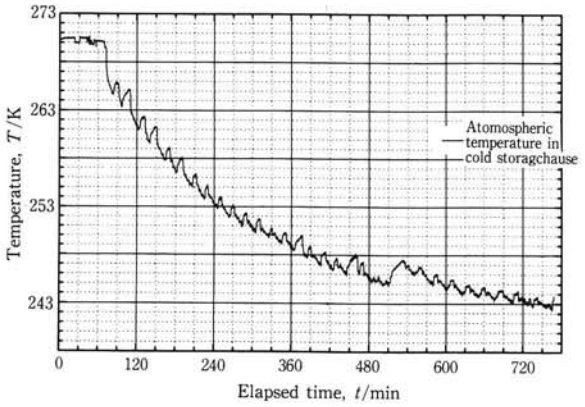

Fig. 14 Change in atomospheric temperature inside 10,000kcal/h class cold storage house while oprating in MH retrigeration mode

developed for refrigeration exhibited the target performance when mounted in a refrigerating system and put into operation, presenting the dynamic properties in line with the P-C-T characteristics obtained in the laboratory.

5. Conclusion

Alloys based on $TiCr_2$ formula was developed for the application as hydrogen absorbing alloys for MH refrigerator. It was made possible to control the equilibrium dissociation chracetristics freely over a temperature range from room temperature to 183 K. The plateau slope of P-C-T diagram could be reduced by replacing with Mn and adding a small amount of Cu, and further made horizontal by homogenizing the composition under the optimal conditions of heat treatment.

When the reaction rate of hydriding reaction at lower temperatures and the durability in cyclic absorption/desorption of hydrogen with the resultant alloys were studied, it was confirmed that adequate reaction rate completing the reaction within 5 minutes or so and excellent durability with 10% aging after 50,000 cycles could be achieved at 213 K.

When a refrigerating system was developed with resultant alloy to examine the performance, the system proved to provide the alloy performance as designed and the refrigerating capability of 243 K.

References

(1) Handbook of Refrigeration and Air-Conditioning, 5th edition, Vol. 4 Refrigerating Apliances, edited by the Japanese Association of Refrigerating Industries (1993), 143. [in Japanese]
(2) Murai: Fresh Food System, 25 (1996), 14. [in Japanese]
(3) Arai: Fresh Food System, 25 (1996), 10. [in Japanese]
(4) J.H.N. van Vucht, FA Kuijpers and H.C.A.M. Brunning: Philips Res. Respts., 25 (1970), 133.
(5) J.J. Reilly and R.H. Wiswall, Jr.: Inorg. Chem., 7 (1968), 2257.
(6) Yamashita, Gamo, Moriwaki and Fukuda: J. Jap. Soc. Met., 41 (1977), 148. [in Japanese]
(7) D. Shaltiel: J. Less-Common Met., 62 (1978), 407.
(8) D. Shaltiel: J. Less-Common Met., 73 (1980), 329.
(9) T. Gamo, Y. Moriwaki, N. Yanagihara, T. Yamashita and I. Iwaki: Int. J. Hydrogen Energy, 10 (1985), 39.
(10) D. Fruchart, J.L. Soubeyroux and R. Hempelmann.. J. Less-Common Met., 99 (1984), 307.
(11) O.Bernauer, J. Topler, D. Noreus, R. Hempelmann and D. Richter: Int. J. Hydrogen Energy, 14
(12) Y. Komasaki, M. Uchida and S. Suda: J. Less-Common Met., 89 (1983), 269.
(13) J.R. Johnson: J. Less-Common Met., 73 (1980), 345.
(14) Kabutomori, Ogawa, Tashirogi and Onishi: J. Jap. Soc. Met., 47 (1987), 157. [in Japanese]
(15) Izumi: J. Jap. Soc. Cryst., 27(1985), 23 [in Japanese]
(16) R. Hempelmann and G. Hilscher: J. Less-CommonMet., 74 (1980), 103.
(17) S. Suda, N. Kobayashi and K. Yoshida: J. Less-Common Met., 73 (1980), 119.
(18) C.N. Park and J.Y. Lee: J. Less-Common Met., 83 (1982), 39.
(19) J.Y. Lee, S.M. Byun, C.N. Park and J.K. Park: J. Less-Common Met., 87 (1982), 149.
(20) V. Shitikov, G. Hilscher, H. Stampfl and H. Kirchmayr: J. Less-Common Met., 102 (1984), 29.
(21) J.Y. Lee, S.M, Byun, C.N. Park and J.K. Park: J. Less-Common Met., 87 (1982), 149.
(22) V. Shitikov, G. Hilscher, H. Stampfl and H. Kirchmayr. J. Less-Common Met., 102 (1984), 29.
(23) P.D. Goodell.. J. Less-Common Met., 99 (1984), 1.
(24) Kabutomori, Takeda, Wakisaka and Onishi: J. Jap. Soc. Met., 59 (1995), 219. [in Japanese]
(25) Murai and Sato: Refrigeration, 71 (1996), 590 [in Japanese]